Geotechnical Engineering Journal of the SEAGS & AGSSEA Vol. 49 No. 2 June 2018 ISSN 0046-5828

State-of-the-Art Research in Geo-energy and Geo-environmental Engineering: Energy Pile and Earthen Capillary Landfill Cover System

Charles W.W. Ng[1], Jason L. Coo[2] & Anthony Gunawan[3]
[1]*Department of Civil and Environmental Engineering, Hong Kong University of Science and Technology, Hong Kong SAR*
[1]*E-mail*: charles.ng@ust.hk

ABSTRACT: Geo-energy and geo-environment are two branches of geotechnical engineering representing current and future grant challenges because of the pressing need to conserve energy and protect the environment. The Hong Kong University of Science and Technology has been actively seeking solutions to these two challenges. The first part (geo-energy) of this paper describes a series of novel cyclic heating and cooling centrifuge tests performed on replacement and displacement floating energy piles installed in both saturated sand and clay. The test results reveal that replacement floating energy piles exhibit ratcheting settlement under a constant working load but at a reducing rate when subjected to temperature cycles, irrespective of the type of soil in which they are embedded. On the contrary, displacement floating energy piles exhibit heave behaviour. No existing theoretical model can capture observed ratcheting pile settlement well. This suggests that care must be taken when designing replacement floating energy piles. In the second part (geo-environment) of the paper, a novel three-layer environmentally friendly earthen cover system for climate regions like Thailand, Indonesia, the Philippines, Malaysia and Singapore is investigated through theoretical examination, physical modelling (e.g., one-dimensional soil column and two-dimensional large flume tests), and advanced numerical simulations. This novel cover system consists of a fine-grained soil underneath a conventional two-layer cover with capillary barrier effects. Two-dimensional water infiltration experiments and numerical simulations show that the newly introduced fine-grained soil layer can greatly minimize rainfall infiltration even after a 4-h rainfall event having a return period of 100 years in climate regions. One-dimensional gas emission tests and numerical simulations reveal that a minimum of 0.6 m thick fine grained soil layer compacted at 10% saturation (e.g. those in arid regions) can adequately satisfy the Australian guidelines. No geomembrane is needed. This new environmentally friendly and robust earthen landfill cover system is thus a promising alternative to other landfill covers for minimizing rainfall infiltration and landfill gas emission under all kinds of weather conditions.

KEYWORDS: Geo-energy, Geo-environment, Energy Pile, Landfill cover system

1. INTRODUCTION

Facing imminent threats such as extreme climate change, and depletion of natural resources, there is increasing awareness on the need to protect and conserve the environment for future generations. Since the 1980s, by the birth of geo-environmental engineering, geotechnical engineers have played an active role in conserving the environment; addressing issues such as waste disposal and the cleaning up of contaminated sites. In recent years, geotechnical field has also gained increasing importance in energy sector, giving birth to another new discipline, i.e. geo-energy. Geo-energy research sought ways to conserve energy by using innovative technology, such as energy piles and energy tunnels. Exploration of alternative energy sources and its safe extraction are also the focus of Geo-energy.

To facilitate exchange of knowledge and ideas, the first International Conference on Geo-energy and Geo-environment (GeGe2015) was held at the Hong Kong University of Science and Technology (HKUST) (Ng et al. 2015a). The second and third GeGe conference will be held in July 2017 and 2019 at Zhejiang University, Hangzhou, China and École Polytechnique Fédérale de Lausanne (EPFL), Switzerland, respectively.

HKUST is one of those pursuing these two trends. For geo-energy aspect, there are ongoing research on soil behaviour under different temperatures as well as energy geostructures, namely, energy pile. Volumetric behaviour of saturated Toyoura sand under thermal cycles was investigated by temperature-controlled triaxial apparatus (Ng et al. 2016a). Cyclic behaviour of unsaturated silt at various suctions and temperatures has also been studied (Ng and Zhou 2014). Volume changes of both intact and recompacted loess under saturated and unsaturated conditions when subjected to temperature cycles have also been studied (Ng et al. 2016b; Ng et al. 2017a). It is obvious that thermal characteristics of soils have profound influence on the performance of energy piles. Ng et al. 2015b investigated the ultimate capacity of energy pile under monotonic heating. Subsequently a new heating and cooling system, capable of operating under high gravity level (i.e. centrifuge application) was built to investigate the effects of thermal cycles on energy pile serviceability (Ng et al., 2014; Shi et al. 2015).

For geo-environmental aspect, HKUST has carried out extensive research relating to landfill cover systems to overcome conventional two-layer cover with capillary barrier effects (CCBE) for arid and semi-arid regions only (Hauser et al. 2001; Zornberg and McCartney 2005; Albright et al. 2004; Bohnhoff et al. 2009). To minimize water infiltration, a CCBE is designed to rely on the contrast of unsaturated permeability between fine-over-coarse grained soil layers. However, during a heavy or prolonged rainfall which is typical in humid climates, matric suction of the coarse-grained soil layer decreases significantly as water reaches the interface of the fine-over-coarse grained soil layer. Once this happens, water can infiltrate through the CCBE because the permeability of the coarse-grained soil is higher than that of the fine-grained soil when it is close to full saturation. In other words, water breakthrough occurs and the CCBE cease to function as intended. More details and explanations are given in section 3.1. Thus, an alternative three-layer earthen capillary barrier landfill cover for use in all-weather conditions (e.g. arid and humid climates) was proposed and investigated using numerical parametric study (Ng et al. 2015c). The factors considered were thickness of the soil layers, rainfall conditions and degree of saturation of the municipal waste. In addition, finite element analyses of coupled water and gas flow were also performed to investigate and compare the performance of three types of landfill covers (i.e., a monolithic compacted clay, a conventional two-layer capillary barrier and a three-layer capillary barrier) regarding gas emission under 34 days of drying (Ng et al. 2015d). It is also commonly known that landfills are a major source of odorous gases, such as hydrogen sulfide (H_2S). To remove these unwanted H_2S, a novel soil conditioner for landfill cover soils was studied using ground granulated blast furnace slag (GGBS) (Ng et al. 2017b; Xie et al. 2017). Moreover, Methane oxidation in landfill covers is a complex process involving water, gas, and heat transfer as well as microbial oxidation. Thus, a new model was developed that incorporates water-gas-heat couple reactive transport in landfill cover soils with methane oxidation (Ng et al. 2015e). Additionally, the effects of nanomaterials as a soil conditioner on the desiccation induced shrinkage and permeability of compacted clay landfill covers were investigated and quantified (Ng and Coo 2014; Coo et al. 2016). The use of biochar-amended clay (BAC) as an alternative material for landfill covers was also investigated by evaluating its gas permeability and soil-water retention characteristics (Wong et al. 2015; Wong et al. 2016). Furthermore, the Ecological performance (e.g., flora and fauna diversities, plant performance and soil properties) of the South East New Territories (SENT) landfill in Hong Kong were monitored during 2000-2012 (Chen et al. 2015).

This paper consists of two main parts. The first part covers the centrifuge results of energy pile under a constant working load subjected to heating and cooling cycles, tested both in saturated clay and sand. For the tests conducted in clay, two piles embedded in different over consolidation ratios (OCRs) are presented (Ng et al. 2014). For the tests conducted in sand, the effect of constructions (i.e. wish-in-place versus jacked-in pile) on energy pile serviceability are presented (Ng et al. 2016c). For the second part of the paper, a new earthen three-layer, environmentally friendly earthen cover system is proposed and verified for minimizing rainfall infiltration and landfill gas emission under all-weather conditions (Ng et. al. 2015f). The feasibility and effectiveness of the proposed earthen cover system are investigated through theoretical examination using unsaturated soil mechanics and physical modelling (e.g., one-dimensional (1D) soil column and two-dimensional (2D) large flume tests). In addition, numerical back-analysis of the experimental results and parametric studies were carried out by varying water permeability of the clay layer to investigate the effects of cracking on the performance of the three-layer cover system. More details are given by Ng et al. (2015g), Ng et al. (2015h), and Ng et al. (2016d).

2. GEO-ENERGY (ENERGY PILES)

2.1 Introduction

Energy pile is a type of Ground Source Heat Pump (GSHP) technology which allows saving of energy for heating and cooling of building. The energy is saved by exploiting the stable ground temperature, which is warmer than air temperature in winter and cooler than air temperature in summer. Therefore, heat exchange with the ground is more efficient than air (Brandl 2006). GSHP is most efficient when there is a balance between heat extracted in winter, and heat injected in summer (Brandl 2016). If energy balance is achieved, in essence, energy is stored in the ground during summer, and extracted to be used for winter. In addition, there will not be any long-term temperature change in the ground, which can lower the efficiency of GSHP. Therefore, this technology is common in temperate climates like Europe, Japan, Korea and America, but not in artic climate like Russia, or tropical countries, such as South East Asian countries (Bi et al. 2009). Some attempts of using GSHP in tropical countries (India and Thailand) are detailed by Soni et al. (2016) and Permchart and Tanatvanit (2009), respectively. In their case studies, the use of GSHP yield 10-15% energy savings, which is significantly less than the energy savings in the UK or US, where 66% and 72% energy savings were recorded, respectively (EEBPP 2000; Omer 2008). In addition to energy efficiency, other hurdles that slows down adoption of energy pile is the possible impact of temperature change to energy pile's serviceability during its operation (Olgun and McCartney, 2014). The latter is the main focus of energy pile research in HKUST.

Operation of energy pile, inevitably results in temperature change to both the pile itself, as well as the surrounding soil. Heating and cooling of energy pile induces axial elongation/shortening and radial expansion/contraction of pile, leading to cyclic compression, extension and shearing on the surrounding soil, and hence volume changes. Consequently, change in horizontal stress, affecting both the capacity as well as the serviceability of energy piles. It is well-known that shaft resistance can be estimated with the equation proposed by Burland (1973), shown in the equation below:

$$\tau_s = (\sigma_h' \pm \Delta\sigma_h') \tan\delta \qquad (1)$$

where, τ_s is the shaft resistance, σ_h' is the horizontal effective stress acting on the pile, $\Delta\sigma_h'$ the change in horizontal effective stress due to operation of an energy pile (i.e., radial expansion and contraction) and δ is the friction angle at pile-soil interface. Further complicating the matter, soil is not thermo-elastic. Figure 1 shows the volumetric response of different materials when subjected to temperature changes. It can be seen that heating of soil does not necessarily induce expansion, unlike most materials which expands linearly when heated (e.g. concrete/steel). With the exception of highly overconsolidated clay, heating followed by cooling of soils result in contraction, and upon further temperature cycles, soil continues to contract at reduced rate (see reconstituted loess in the figure). It is obvious that this temperature induced volume change in soil adjacent to an energy pile can alter the horizontal stress ($\Delta\sigma_h'$) acting on the pile, affecting its shaft resistance, and hence pile settlement.

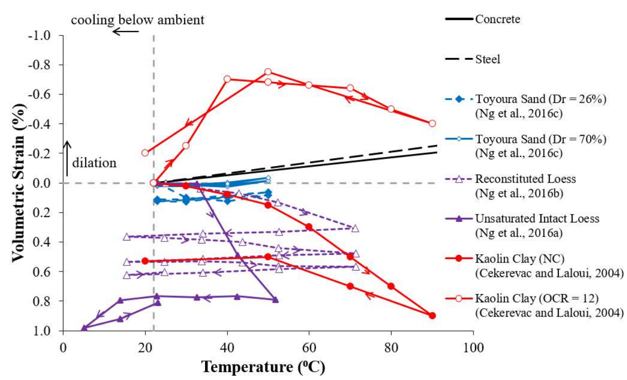

Figure 1 Volumetric changes with respect to temperatures of different materials

In this paper, centrifuge modelling of floating replacement and displacement energy piles embedded in saturated Toyoura sand (Ng et al. 2016c) and floating replacement energy piles in saturated Kaolin clay (Ng et al. 2014) with different overconsolidation ratios (OCR) subjected to thermal cycles are presented.

2.2 Centrifuge modelling of floating energy piles

As soil is a stress-dependent material, conducting physical model test at 1g condition may not give representative results to that in the field. The fundamental principle of centrifuge modelling is to recreate the stress condition similar to that in field, thus allowing engineering problems to be studied at a smaller scale. By subjecting a model to an enhanced centripetal acceleration (Ng, where N is the gravitational force multiplier), a prototype problem can be modelled according to scaling laws (Taylor 2004). Table 1 shows the relevant scaling for centrifuge modelling of energy piles.

For example, using the scaling law for length, under 40g, a 50 mm long model pile can simulate a 20 m long pile in prototype. Particularly, the scaling laws for heat conduction is N^2 (Krishnaiah and Singh 2004), meaning that the time taken to investigate temperature effect is N^2 time faster than that in field test, thus simulation of long-term behaviour of energy piles can be carried out in a much shorter time than that in field.

The centrifuge model tests reported here were all conducted under 40g at the Geotechnical Centrifuge Facility (GCF) of Hong Kong University of Science and Technology (Ng 2014).

Table 1 Relevant scaling laws

Parameter	Prototype-model ratio
Acceleration	1/N
Temperature	1
Time (diffusion)	N^2
Length	N
Density	1
Stress	1
Strain	1
Displacement	N
Mass	1
Axial rigidity	N^2

2.2.1 Experimental Programme

Two series of model pile tests were conducted in saturated Toyoura sand and Kaolin clay. In the former series, one model energy pile was installed in two separate compartment (EP-SR and EP-SD). The aim of the first series was to investigate construction effect on the serviceability of energy pile. EP-SR was used to model replacement pile, i.e. bored pile; while EP-SD was used to model displacement pile. For EP-SR, the pile was wished-in-place at the design depth, while EP-SD was wished-in-place 3*D* (pile diameter) shallower than EP-SR. For EP-SR, working load was initially applied, followed by 5 thermal cycles. As for EP-SD, the pile was initially driven by 3*D* to the same depth as EP-SR, then unloaded to the same working load as EP-SR, finally the same thermal cycles were applied to EP-SD.

In the second series, two clay models with different OCRs were prepared in two different compartments. Each clay model contained two piles, a reference and an energy pile, RP-C1 and EP-C1 in the first compartment, and RP-C2 and EP-C2 in the second compartment. The reference pile was used to obtain the working load to be applied on the respective energy pile. Similar to the series in sand, the model energy piles were initially subjected to their respective working load, followed by 5 thermal cycles. The aim for the second series were to investigate the serviceability of energy piles installed in soil with different OCRs.

2.2.2 Experimental setup and instrumentations

Figure 2 shows the elevation views of the centrifuge model package for the series in sand. The model container used had a dimension of 1245 x 350 x 850 mm (length x width x height), which corresponds to 49.8 x 14 x 34 m in prototype scale. The model compartment was partitioned into two equal compartments, each about 600 mm long. The side walls and base of the container was insulated with 18 mm-thick wooden boards. One model energy pile was installed in each compartment (EP-SD and EP-SR). Both model piles had a diameter (*D*) of 22 mm and a length (*L*) of 600 mm (0.88 m and 24 m in prototype). The model energy pile in the right compartment (EP-SR) was embedded to 420 mm depth (16.8 m in prototype); the left pile (EP-SD) was initially wished-in-place to 354 mm depth (14.2 m in prototype; initial position shaded in grey), which was 3D shallower than the designated depth. The pile was instrumented with thermocouples at 60 mm intervals, starting from 20 mm above the pile toe. Additional instrumentation includes thermocouple trains (TT-S1 and TT-S2), with thermocouples (TCs) attached at 100 mm interval. TT-S1 and TT-S2 were installed 50 and 40 mm (2.0 and 1.6 m in prototype) away from the centre of EP-SR and EP-SD, respectively. The different distances were chosen in order to obtain temperature distribution at different distances.

Figure 3 shows the elevation views of the centrifuge model package for the series in clay. For this series, the same model container, partitions and wooden insulators were used. A sand bed of 60 mm thick was placed at the bottom of container to provide drainage. Two model piles were installed in each compartment (RP-C1, EP-C1, RP-C2 and EP-C2). All piles were embedded to the same depth as EP-SR from the sand test, i.e. 420 mm (16.8 m in prototype). The diameter of the piles was also identical to the sand series, i.e. 22 mm (0.88 m in prototype). The piles were also instrumented with thermocouples at 60 mm interval, starting 20 mm from the pile toe. Similar to the sand series, a thermocouple train, was installed 30 mm away from the centre of each energy pile (TT-C1 for EP-C1 and TT-C2 for EP-C2). The interval of the thermocouples was 120 mm, starting 50 mm from the ground surface.

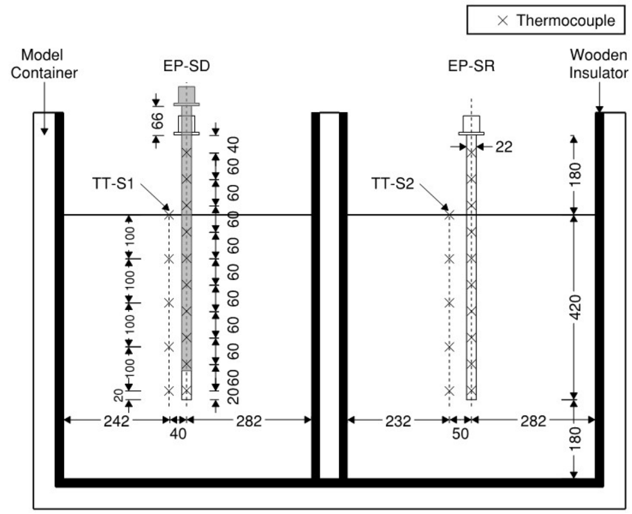

Figure 2 Schematic diagrams of centrifuge model package in sand (Ng et al. 2016c)

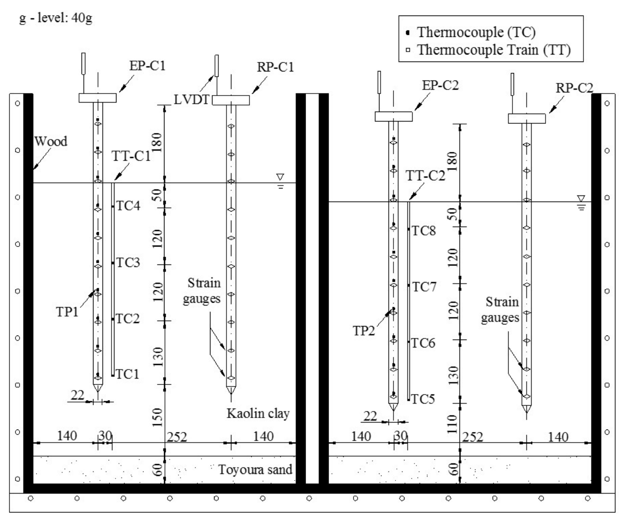

Figure 3 Schematic diagrams of centrifuge model package in clay (Ng et al. 2014)

2.2.3 Model preparation

For the tests in sand, drainage pipes were initially installed at the base of the wooden insulators. Then, the two energy piles and thermocouple trains were fixed at their designated position by temporary frames. Toyoura sand was then poured from a constant height of 1000 mm, by using a sand hopper, yielding an average relative density of 69%. This essentially modelled 'bored' pile for EP-SR; the construction sequence for EP-SD is described later. The model container was then sealed to allow application of suction to facilitate saturation. Finally, de-aired water was supplied from the bottom drainage pipes to saturate the sand.

For the tests in clay, likewise, drainage pipes were initially installed at the base of the wooden insulators, and sand was rained in similar manner as described above, to cover the drainage pipes (60 mm thick). Next, clay slurry was placed above the sand layer. Steel plate was then placed above the clay slurry for application of surcharge. The sample was consolidated at 40g with a surcharge of 82 kPa (for the left compartment) and 450 kPa (for the right compartment). After the consolidation process, the centrifuge was spun down, and the surcharge was removed. This was done to prepare clay sample with different OCRs. This process yielded OCR of 1.7 at the pile toe for the lightly overconsolidated clay (left compartment), and OCR of 4.7 at the pile toe for the heavily overconsolidated clay (right compartment). Finally, boreholes were excavated to the designated depth, and the model piles were installed to the pre-drilled boreholes.

2.2.4 Heating and cooling system

The heating and cooling system used was developed at the Hong Kong University of Science and Technology. The system is mounted on the centrifuge arm and operates under high-*g*. Ethylene glycol, the heat-exchange fluid used, is sent down from the system to the model pile by way of insulated tubing. For more details on working principles one can refer to Shi et al. (2015).

2.2.5 Test procedure

For the tests in sand, once the model preparations were completed, the centrifuge was spun to 40g. For EP-SR, a working load of 800 kN was applied (corresponding to FoS = 1.8 according to Ng et al. (2001) failure criterion). The working load was maintained for 2 hours (4.4 months in prototype), and then the heating and cooling cycles were initiated. Each heating and cooling phase last for 108 minutes (4 months in prototype). A total of five heating and cooling cycles were applied. Upon completion of the thermal cycles, the pile temperature was returned to the ambient temperature. For EP-SD, to model pile driving, the pile was loaded incrementally in-flight until the pile settles by 300% *D*, reaching the same depth as EP-SR. The final driving load was 7200 kN. EP-SD was then unloaded to the same working load of 800 kN. Thereafter, the same time was allowed to pass before the five heating and cooling cycles were applied.

For the tests in clay, after the centrifuge was spun to 40g, the clay was reconsolidated up to 90% degree of consolidation (Asaoka 1978). After the target degree of consolidation was reached, the reference piles (EP-C1 and EP-C2) were loaded with a constant displacement rate in undrained conditions based on Finnie (1993) criterion. The ultimate pile capacity was then derived using failure criterion proposed by Ng et al. (2001). A factor of safety of 2.5 was chosen and a working load of 96 kN and 192 kN were applied on EP-C1 and EP-C2, respectively. Similar to the tests in sand, the working load was maintained for 2 hours before the heating and cooling cycles were applied. The duration of heating and cooling phases were the same to that of the tests in sand.

2.3 Results and discussion

All the data presented hereafter are expressed in prototype scale unless stated otherwise.

2.3.1 Temperature history

Figure 4 shows the temperature history of EP-SR, at 6.4 m below the ground surface. The soil temperature, measured 8 m below the ground surface and 2 m away from the pile centre was also included. From the figure, it can be seen that EP-SR experienced a maximum temperature of 29 ºC, and a minimum temperature of 15 ºC. Therefore EP-SR experienced thermal cycles with amplitude of ±7 ºC. The temperature history of EP-SR is typical to all 4 model energy piles tested (EP-SR, EP-SD, EP-C1, EP-C2), thus for brevity they are not included in this paper. Only the thermal cycles amplitude for the other three piles are reported in this paper.

For EP-S2, the thermal cycles experienced was also with amplitude of ±7 ºC, while EP-C1 and EP-C2 experienced thermal cycles with amplitude of ±10 ºC. For the rest of the model pile temperature history, one can refer to Ng et al. (2014; 2016c).

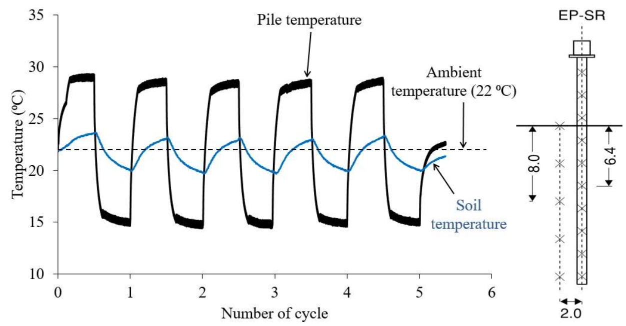

Figure 4 Temperature history of EP-SR

2.3.2 Pile head displacement with thermal cycles

Figure 5 shows the pile head displacement (normalized with pile diameter), against number of thermal cycles. For the replacement pile in sand (EP-SR), the pile initially experienced slight heave (about 0.2% *D*) during the first heating phase, but after the first cooling phase, significant settlement was observed (up to 2% *D*). This settlement was not recovered upon the second heating phase. Subsequent thermal cycles resulted in a ratcheting displacement pattern but at a reducing rate. This settlement is a result of thermal-induced contraction of sand (see Figure 1) as well as cyclic shearing on the surrounding soil, resulting in reduction of horizontal stress, as expressed in equation 1 (Ng et al. 2016e).

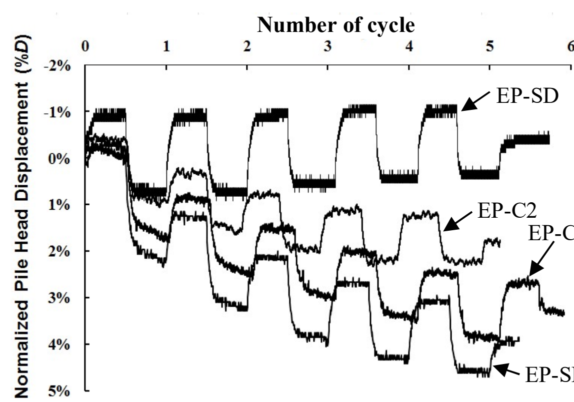

Figure 5 Normalized ratcheting pile head displacement with temperature cycles

In contrast, EP-SD did not experience any cumulative settlement. In fact, after the five thermal cycles, slight heave was measured (0.4% *D*). This could be due to the densification effect of the surrounding soil when EP-SD was jacked in (Simons and Menzies 2000), which counteracted the two mechanisms that cause pile settlement during thermal cycles. As shown in Figure 1, sand with higher relative density undergoes lower thermal contraction than its looser counterpart. Secondly, due to the densification effect, when the surrounding soil was sheared, the soil dilated, instead of contracting, resulting in the final observed heave. In addition, the increase in horizontal stress due to pile driving maybe higher than the reduction induced due to thermal cycles.

For the two piles in clay, EP-C1 and EP-C2, ratcheting displacement pattern but at a reducing rate was also observed. After the application of 5 thermal cycles, EP-C1 settled by about 3.5% *D*, while EP-C2 settled by about 2%*D*. The difference in the magnitude of settlement is due to thermal behaviour of clay. As shown in Figure 1, clay which is normally consolidated contracts, while clay with high OCR dilates. Therefore, the surrounding clay of EP-C1, which is of lower OCR than EP-C2, contracts more, resulting in higher magnitude of settlement.

Although a new cyclic thermo-mechanical model for unsaturated soil has been developed by using the bounding surface plasticity theory (Zhou & Ng, 2016) to allow plastic strain inside the bounding surface, it remains a significant challenge to simulate the observed ratcheting pile head settlement precisely. Recently Ma et al. (2017) has proposed an alternative approach to model volume change of fine-grained soil subjected to thermal cycles. Limited success has been reported.

2.4 Summary and conclusions for floating energy piles

A number of centrifuge model tests on floating energy piles were carried out to investigate potential serviceability problem that floating energy piles supported structures may experience. Different conditions, such as construction effects, as well as soil type and state were investigated. From the two series of tests, the following conclusions can be drawn:

1. For replacement energy piles, thermal cycles induced ratcheting settlement pattern but at a reducing rate. For displacement energy piles, slight ratcheting heave was observed instead.
2. The magnitude of thermal cycles-induced settlement varies with soil type and state. Energy pile embedded in medium overly consolidated clay settles less than energy pile which was embedded in lightly over consolidated clay.
3. The displacement energy pile test in sand also implies that energy pile installed in denser sand settles less than energy pile installed in loose sand.
4. From the results, ground improvement might be required for energy piles that were to be installed in loose sand or normally consolidated clay.

3. NEW THREE-LAYER EARTHEN COVER SYSTEM

3.1 Theoretical considerations of the newly proposed landfill cover

Schematic diagrams of a two-layer CCBE and the proposed landfill cover are compared in Figure 6. As shown in Figure 6a, CCBE contains two soil layers which are a fine-grained soil layer overlying a coarse-grained soil layer. It relies on the capillary barrier effects between these two soil layers to minimize water infiltration. However, due to water breakthrough of the coarse-grained soil layer at high water contents, CCBEs are not suitable for humid climates. More explanations are further given in section 3.1.1. Comparatively, the newly proposed landfill soil cover is a three-layer cover system, which consists of a compacted clay layer, a coarse-grained layer and a fine-grained layer, compacted successively from the bottom to the top of the system, as shown in Figure 6b. According to the water permeability functions illustrated in Figure 7, by introducing a compacted clay layer beneath a CCBE, infiltrated water through the upper two-layer can be intercepted and reduced by the bottom clay layer which has lower water permeability at high degree of saturation (i.e., low suction) in humid climate. On the other hand, the bottom clay layer can be protected by the upper two soil layers from desiccation during dry seasons because the upper two soil layers have low water permeability at high suctions (i.e., low relative humidity). Another key feature of this proposed landfill cover is to prevent excessive landfill gas emission due to the high air-entry value of the clay layer.

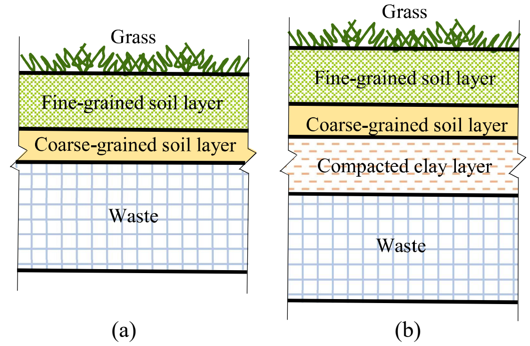

Figure 6 Conceptual diagrams of landfill covers: (a) conventional capillary barrier landfill cover; (b) Newly proposed landfill cover

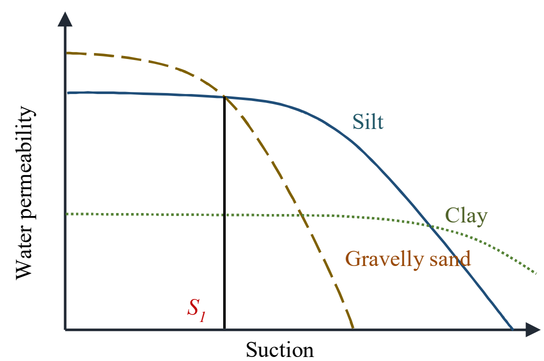

Figure 7 Schematic diagram showing water permeability functions of silt, gravelly sand, and clay

3.1.1 Principle of reducing water infiltration

Figure 7 shows a schematic diagram illustrating relationship between water permeability and matric suction of each soil layer. Matric suction is defined as the difference between pore gas pressure and pore-water pressure in a soil. When a soil becomes drier and water content decreases, the suction and water permeability increases and decreases, respectively (Ng and Menzies 2007).

i When soil suction in the three-layer landfill cover is larger than point S_1 (shown in the figure), i.e., at semi-arid or arid climates, cover soils are relatively dry. Water permeability of silt layer is much higher than that of gravelly sand layer. Infiltrated water stores in the silt layer and flows away in this layer, but no water infiltrates into the gravelly sand layer. In other words, the two-layer CCBE works.

ii. When soil suction in the landfill soil cover is less than point S_1 (shown in the figure) under heavy or prolonged rainfalls, i.e., at humid climates, cover soils are nearly saturated or saturated. Water permeability of gravelly sand layer is the highest while that of clay layer is the lowest. Capillary barrier effect formed by upper silt layer and underlying gravelly sand layer will lose its function and water infiltrates into the gravelly sand layer, since the water permeability of gravelly sand layer is higher than that of silt layer. At this point, the infiltrated water is prevented by the clay layer due to its lowest water permeability and may be drained away through the gravelly sand layer due to its relatively high saturated permeability. In this way, the head of water on the underlying clay layer is reduced and thereby the amount of water percolation will be minimized.

The addition of the compacted clay layer underlying the CCBE makes the proposed landfill cover applicable to any weather conditions.

3.1.2 Principle of preventing gas emission

Figure 8 shows the relationship between gas flow rate and landfill gas pressure of each soil layer in the cover system. When landfill gas pressure is relatively low, gas flow rate in the cover system is almost zero. When landfill gas pressure is larger than the limiting breakthrough gas pressure (at point A) of the clay layer, landfill gas flow rate increases rapidly. This limiting breakthrough pressure at which landfill gas starts to enter into soil rapidly is also called air-entry value. When the level of landfill gas pressure is less than A, landfill gas cannot penetrate into the clay layer. The landfill gas pressure is generally less than 10 kPa in the field (McBean et al. 1995). Since the limiting breakthrough gas pressure (i.e., air entry value) of the clay layer is larger than typical landfill gas pressure, landfill gas will not breakthrough. Therefore, the cover system can prevent landfill gas emission.

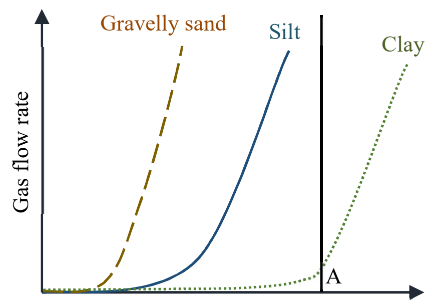

Figure 8 Schematic diagram showing relationship of gas flow rate and landfill gas pressure of silt, gravelly sand, and clay

3.2 Physical modelling

3.2.1 Experimental program, test apparatus and test materials

To evaluate the performance of the proposed three-layer landfill cover in minimizing water infiltration and gas emission, 1-D soil column and 2D flume tests were carried out.

Figure 9 shows a typical schematic diagram of the soil column used for the 1D water infiltration, gas breakthrough and gas emission test. The total height of the soil column is 1300 mm with an inner diameter of 140 mm. The soil column was instrumented with tensiometers, heat dissipation matric potential sensors, pore air pressure transducers and moisture probes to monitor the variations of pore water pressure, water content and pore air pressure with depth. The amount of water volume infiltrated and gas emission rate into and out of the soil was also monitored throughout a test. For the water infiltration test, silt, gravelly sand, and kaolin clay were used to model the three-layer landfill cover system. For the gas breakthrough and gas emission test, clay was used with consideration of four degrees of saturation (40%, 60%, 80% and 100%) and two clay thicknesses (0.4 m and 0.6 m). The basic properties of these three soils are shown in Table 2.

Figure 10 shows a photograph of the flume model box for the 2D water infiltration test. The flume model box has dimensions of 3 m (length) x 1.5 m (height) x 1 m (width). A rainfall simulation system was placed above the flume model box to create rainfall with a constant intensity. The flume model box was heavily instrumented with tensiometers, moisture probes and drain gauges to monitor pore water pressure, water content, surface runoff, infiltration and lateral drainage of each layer, and percolation of the cover system. Similarto the 1D water infiltration test, silt, gravelly sand, and kaolin clay was used to model the three-layer landfill cover system.

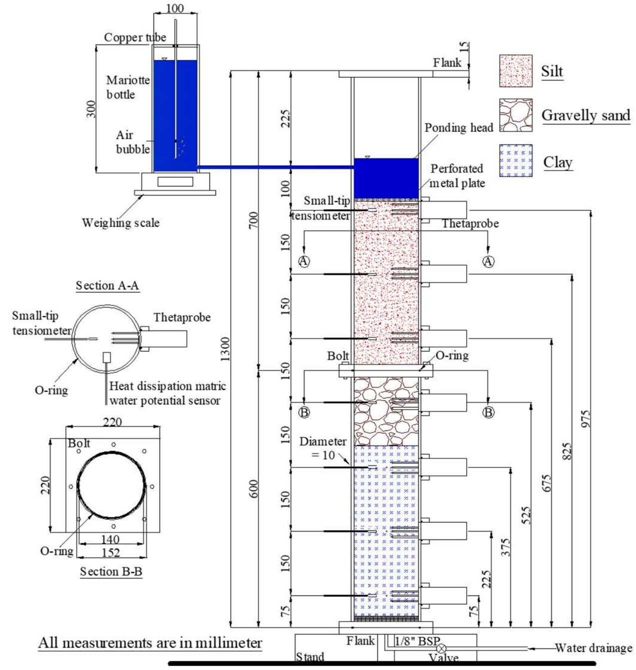

Figure 9 Schematic diagram of the soil column

Table 2 Basic properties of the silt, gravelly sand and clay

Description	Silt	Gravelly sand	Clay
Unified soil classification system (USCS)	ML	SP	CH
Specific gravity, G_s	2.61	2.62	2.52
Liquid limit, LL	22	-	59
Plastic limit, PL	16	-	32
Plasticity Index, PI	6	-	27
Maximum dry density, ρ_d (kg/m^3)	1771	1494	1264
Optimum moisture content (%)	14	-	36
Saturated permeability, k_s (m/s)	1.4×10^{-6}	9.7×10^{-3}	5.7×10^{-9}

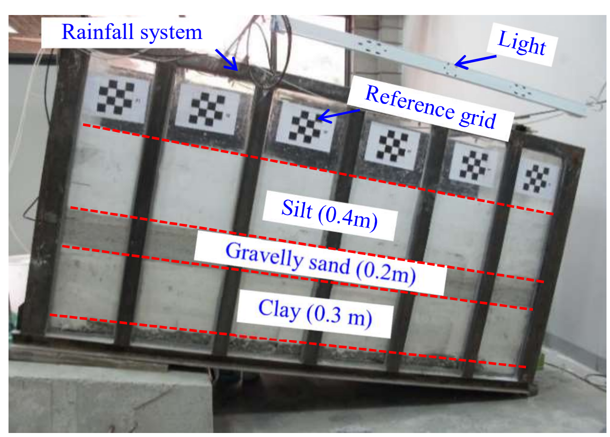

Figure 10 Layout of the inclined flume model

Water retention curve (WRC) is the relationship between volumetric water content and suction of soil. WRC is an important hydraulic parameter of unsaturated soil. In this study, both the wetting and drying WRCs of the three soils used in this study were obtained by using modified pressure plate apparatus (Ng and Pang 2000). the wetting WRC data is fitted using the van Genuchten (1980) WRC equation. The WRC data and the fitted curves are shown in Figure 11.

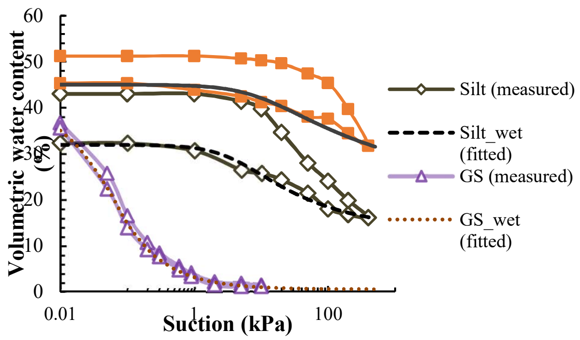

Figure 11 Measured and fitted WRCs of silt, gravelly sand (GS) and clay

3.2.2 Sample preparation and test procedures

For the 1D water infiltration test, the three soil layers, namely, a clay layer, a gravelly sand layer and a silt layer, were compacted successively from bottom to the top of the cover system. The thickness of each soil was 0.4 m, 0.2 m and 0.4 m for clay, gravelly sand and silt, respectively. The soils were initially mixed with water to reach the optimum moisture content as given in Table 2. The soils were then compacted to their targeted degree of compaction (DOC) or relative density (RD) which is 95 DOC, 95 RD and 90 DOC for clay, gravelly sand and silt, respectively. The different sensors were then installed and allowed to equalize with the soil. After sensor equalization, 0.1 m constant head ponding was applied on the soil surface using a constant-head water supply system. The bottom valve was opened to allow any percolation to drain out. Most engineering design guidelines are based on rainfall return period (GEO 2011). Rainfall return periods at various ponding duration are back-calculated by using the relationship between rainfall depth and duration according to the “Hong Kong Stormwater Drainage Manual” (DSD 2013). Further details regarding the conversion of equivalent rainfall return period are given in Ng et al. (2016d).

For the 2D water infiltration test, the three soil layers, namely, a clay layer, a gravelly sand layer and a silt layer, were compacted successively from bottom to the top of the cover system. The thickness of each soil was 0.3 m, 0.2 m and 0.4 m for clay, gravelly sand and silt, respectively. During compaction, the drain gauges were buried within each layer. After compaction, the flume model box was inclined at 10 degrees and the different sensors were installed through the holes and connectors in the back sidewall. Soils in landfill covers in the field have undergone many wetting and drying cycles. In order to simulate field conditions, the three-layer landfill cover system was first subjected to three cycles of wetting and drying prior to the model test. In order to simulate the worst initial condition, a heavy rain event of 1 in 100 year return period was chosen for the wetting event. After the three cycles of wetting and drying, the pore water pressure distribution in gravelly sand and silt layer followed the hydrostatic line. Subsequently, rainfall was applied at the intensity of 73.8 mm/h for 4 h to simulate an extreme rainfall event having a return period of 100 years in Hong Kong. After the rainfall event, the flume box was left exposed to the laboratory ambient conditions (i.e., temperature of 20 ± 5 °C and humidity of 60 ± 10%) for 20 h, which resulted in an average evaporation rate of $3.3\text{x}10^{-8}$ m/s.

For the 1D gas breakthrough and gas emission test, two methods were used to prepare the kaolin clay samples, depending on their degree of saturation. For the tests at degrees of saturation of 40%, 60% and 80%, oven-dried kaolin clay powder was initially mixed with de-aired water to reach the target water content. After that, the clay was then compacted to the targeted DOC of 90 with thickness of either 0.4 m or 0.6 m. For the tests at degree of saturation of 100%, the clay samples were first prepared at the optimum water content. Then, each sample was subjected to bottom-up saturation to achieve degree of saturation of about 100%. For the gas breakthrough tests, after soil preparation, a constant gas pressure of 5 kPa was applied at the base of the soil column for 3 days. If no gas breakthrough occurs, gas pressure was increased from 5 to 10 kPa and then maintained at that value for another 3 days. Then, gas pressures of 15, 20, 30, 40 and 50 kPa were subsequently applied to the soil sample until gas breakthrough occurs. For the gas emission rate tests, after soil preparation, constant gas pressures were applied at the bottom of the soil column until a stable gas flow is achieved. When a gas pressure of 1 kPa was finished, the gas pressure was increased to 5 kPa and then kept constant until a stable gas flow is achieved. Then, 10 and 20 kPa gas pressures were applied by following a similar procedure.

3.3 Numerical back analysis and parametric study

In order to enhance the fundamental understanding of the experimental results, a finite element analysis was carried out to back-analyse the model tests. The computer code used to perform the numerical analysis was CODE_BRIGHT. This software can be used to simulate both saturated and unsaturated flows under steady and transient conditions. The governing equations for simulating water-gas coupled flow are given as follows:

$$\begin{cases} \phi \dfrac{\partial(\theta^{w} S_{w})}{\partial t} + \nabla(j^{w}) = 0 \\[2ex] \phi \dfrac{\partial[\theta^{g}(1-S_{w})]}{\partial t} + \nabla(j^{g}) = 0 \end{cases} \tag{2}$$

where ∇ is the gradient of a vector field; ϕ is porosity; θ is mass content per unit volume of phase; S_w is soil water degree of saturation; and j is total mass flux. Superscripts w and g refer to water and gas, respectively. More details of the software were reported by Olivella et al. (1994).

It should be pointed out that the variable j^w and j^g in Equation 2 are dependent on the water permeability and gas permeability of soil, respectively. In this study, the permeability functions are predicted from the wetting WRC of the soil using in conjunction the van Genuchten-Mualem equation (van Genuchten 1980; Mualem 1976). The boundary conditions and numerical modelling procedures adopted are identical to those used in the physical tests. The initial conditions of the numerical simulations were obtained by specifying initial measured pore water pressure distributions obtained from the experiment.

In the field, the water permeability of clay may increase due to desiccation cracks and differential settlement (Albright et al. 2006). Hence, a parametric study was carried out by increasing the saturated clay permeability up to three orders of magnitude (i.e., k_s = $3\text{x}10^{-9}$ m/s to $1\text{x}10^{-6}$ m/s) to investigate the effect of cracking on the performance of the three-layer cover system under 1D and 2D water infiltration.

To improve our understanding on the influence of soil moisture on gas emission through unsaturated compacted clays, the degree of saturation was extended to a wider range of 10% to 100%. This simulates different weather conditions in the field. Gas pressure of 5 kPa which represent the average typical landfill gas pressure was selected in the simulation.

3.4 Interpretation of results

3.4.1 Distribution of pore water pressure profile for the 1D water infiltration test

Figure 12 shows both computed and measured pore water pressure profiles, which were obtained from the numerical and measured results of the soil column water infiltration test. The numerical simulation results show a good agreement with those observed in the laboratory experiments. Upon application of 0.1 m constant ponding head for the first 4 hours (4 year rainfall), infiltration occurred mainly in the silt layer but not in the gravelly sand layer as reflected by the fact that measured and simulated pore water pressure remained unchanged in the gravelly sand layer. In other words, the gravelly sand layer served as a capillary barrier and impeded the downward flow of water due to its relatively low permeability at higher suction range. However, the capillary barrier effect was not sustained for a long time when water infiltration continued in the silt layer. As a result, at elapsed time of 8 hours (530 year rainfall), measured pore-water pressure at the gravelly sand layer suddenly increased from -20 kPa to -2 kPa, which is consistent with the computed pore water pressure from the numerical simulation. The sudden increase in pore-water pressure indicated that during the period between 4 to 8 hours, water is observed to infiltrate freely into the gravelly sand layer after a total breakthrough of suction value is achieved after continuous water infiltration (Ross 1990; Yang et al. 2006). The two-layer CCBE was no longer effective after this event occurred. This entails that capillary barrier has a temporary effect in restricting the downward movement of water, as evidenced by the change in pore water pressure measurements across the fine-coarse soil interface. When water was continuously applied to the soil surface, breakthrough at the soil interface would eventually occur under the one-dimensional condition. This phenomenon has been demonstrated by numerous researches for two-layer CCBEs (Stormont and Anderson 1999; Parent and Cabral 2006; Lee et al. 2011). Due to continuous application of ponding it can be observed that after 24 hours a hydrostatic condition seems to develop above the clay layer. After 48 hours of ponding (>100 year rainfall), both simulated and measured results demonstrate that only the upper portion of the clay layer shows an increase of pore water pressure. It is also noted that no percolation was measured. This indicates that due to the addition of clay layer underneath a two-layer CCBE, infiltrated water requires a rather long duration to reach the deeper portion of the clay layer. Thus, percolation can be prevented even for rainfalls greater than 1000 year return period.

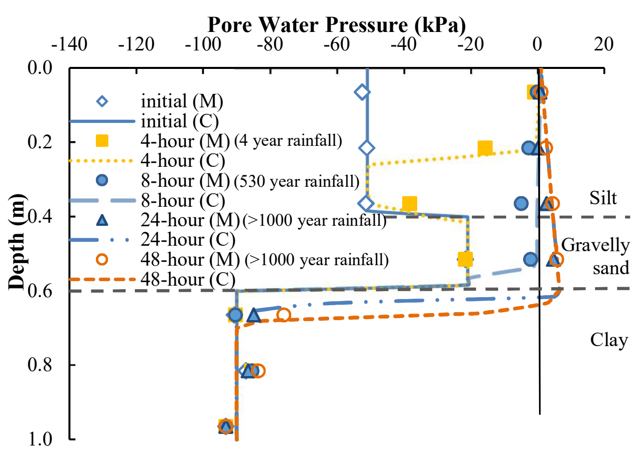

Figure 12 Measured (M) and computed (C) pore water pressure distributions during 1D water infiltration

3.4.2 Distribution of pore water pressure profile for the 2D water infiltration test

Figure 13 shows the measured and computed profiles of pore water pressure during and after the extreme rainstorm of the flume model. The numerical simulation results are fairly consistent with the measured values. The maximum difference is about 2 kPa. Initially (i.e., t = 0-hour), the measured pore water pressure ranged from -5.5 kPa to -2.5 kPa along the depth in the two upper layers. The hydraulic gradient was close to that of the hydrostatic line. This indicates that water initially stored in the silt layer because of the capillary barrier effect (Ross 1990). Beneath the two upper layers, the pore water pressure in the clay layer was negative. The larger the depth, the smaller the pore water pressure. During the first half-hour of rainfall, the measured pore water pressure in the silt layer increased from -5.5 kPa to -4.0 kPa at the depth of 0.1 m and from -3.4 kPa to -2.0 kPa at the depth of 0.3 m. In the gravelly sand layer, the measured pore water pressure increased from -2.8 kPa to -2.7 kPa. At this stage, the gravelly sand layer was acting as a capillary barrier. In other words, no breakthrough occurred in the two upper layers. Under these two layers, the measured pore water pressure in the clay layer varied from -16.0 kPa to -15.7 kPa at the depth of 0.7 m and from -84.5 kPa to -84.4 kPa at the depth of 0.8 m. During the subsequent three and a half-hour of rainfall, the measured pore water pressure in the silt layer increased to about 0.2 kPa. The measured pore water pressure in the gravelly sand layer increased to -1.3 kPa at 1-hour and to -0.5 kPa at 1.5-hour. This indicates that the rainwater had infiltrated into the gravelly sand layer at 1–1.5-hour. In other words, breakthrough occurred. Under the two upper layers, the pore water pressure in the clay layer increased from -15.7 kPa to -14.9 kPa at the depth of 0.7 m and from -84.4 kPa to -83.6 kPa at the depth of 0.8 m at 1–4-hour. This suggests that almost no water infiltrated the clay layer because of its low permeability. In other words, the effectiveness of the three-layer landfill cover system in humid climates was satisfactory because of the addition of the clay layer. During the evaporation following the rainfall event (4–24-hour), the pore water pressure of the two upper layers returned to their original levels. In the clay layer, the pore water pressure at the depth of 0.7 m remained negative.

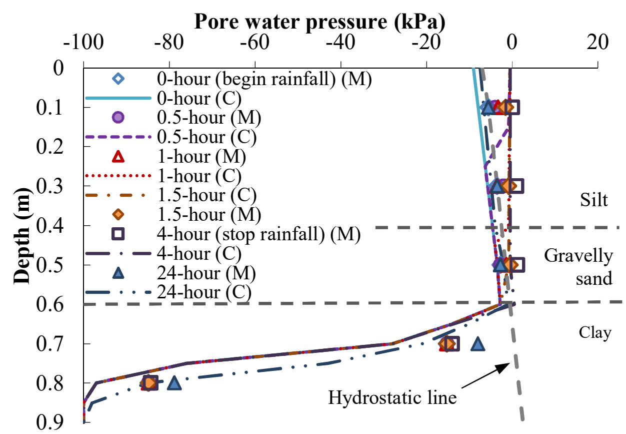

Figure 13 Measured (M) and computed (C) pore water pressure distributions during 2D water infiltration

3.4.3 Influence of clay saturated permeability on percolation

Figure 14 shows the computed percolation of the three-layer cover system with different clay saturated permeability under 2D water infiltration. As expected, the percolation increased with the increase of clay saturated permeability, particularly when it was larger than 1×10^{-8} m/s. When the saturated permeability further increased to 1×10^{-6} m/s, the percolation increased to as large as 20 mm, i.e. about 7% of the precipitation. Based on the relationship between percolation and saturated permeability of clay, a critical permeability could be identified as the point at which the percolation began to increase significantly. In this study, the critical permeability was about 1x10^{-8} m/s. Below this critical value, the influence of saturated permeability on percolation was negligible. When the saturated permeability increased from 10^{-9} m/s to 10^{-8} m/s, the percolation only increased by about 0.8 mm, which is less than 0.3% of the precipitation. Beyond this critical value, the percolation increased significantly from 0.8 mm to 19.2 mm as the saturated permeability increased from 10^{-8} to 10^{-6} m/s. The results of this parametric study suggest that the performance of the three-layer landfill cover may deteriorate if the clay saturated permeability is higher than 1x 10^{-8} m/s induced by cracking.

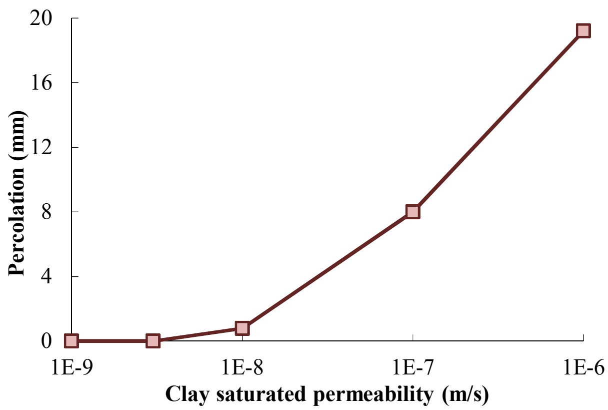

Figure 14 Influence of clay saturated permeability on percolation under 2D water infiltration

3.4.4 Gas breakthrough pressure at different degrees of saturation

Figure 15 shows the measured relationship between applied gas pressure and gas flow rate at three different clay degrees of saturation (60%, 80% and 100%). The figure clearly reveals two types of soil response. At degree of saturation of 60% and 80%, the gas flow rate is almost zero in the lower range of gas pressure. When the gas pressure reaches a threshold value, the gas flow rate suddenly increases.

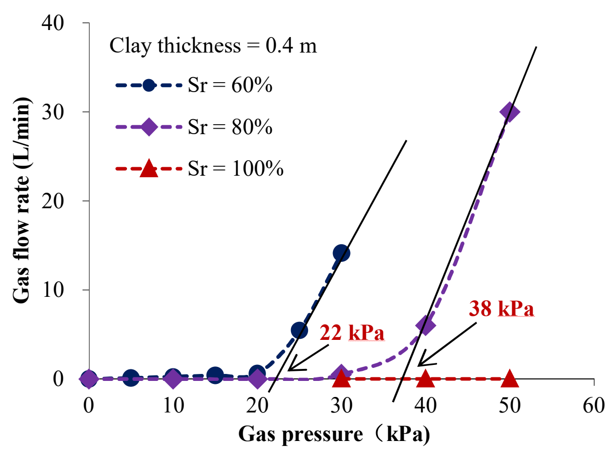

Figure 15 Measured relationship between applied gas pressure and gas flow rate at three degrees of saturation (clay thickness = 0.4 m)

The threshold value is defined as gas breakthrough pressure. It can be seen from the figure that gas breakthrough pressure is estimated to be 22 and 38 kPa at degree of saturation of 60% and 80%, respectively. On the other hand, for the test at degree of saturation of 100%, gas flow rate is almost zero in the whole range of gas pressure (0–50 kPa). This suggests that gas breakthrough pressure is higher than 50 kPa at this testing condition. Comparisons between the three curves illustrate that the gas breakthrough pressure increases with increasing degree of saturation. The influence of degree of saturation is most likely because more pores are occupied by soil water in the compacted sample at higher degree of saturation. A higher pressure is therefore required to form an interconnected air-filled channel for gas flow.

3.4.5 Gas emission rates at different degrees of saturation and clay thickness

Figure 16 shows the comparison between measured and computed gas emission rates at two different clay thickness (H = 0.4 m and 0.6 m) with applied gas pressure of 5 kPa. Good agreements are observed between the measured and computed results. The maximum gas emission rate allowed by the Australian guideline (CFI 2013) is also included for comparison. Both measured and computed results reveal that gas emission rate decreases significantly with an increase of degree of saturation. Furthermore, the computed results clearly illustrate that the relationship between gas emission rate and degree of saturation is quite non-linear. Under low degree of saturation (less than 60%), gas emission rate slightly decreases when degree of saturation increases. On the contrary, when degree of saturation further increases above 60%, gas emission rate drops rapidly. This may be because pore air in unsaturated clay translates from a continuous phase to an occluded phase (Tanai et al., 1997).

From the computed results, it can be seen that the difference of gas emission rates between H = 0.4 m and 0.6 m becomes smaller as degree of saturation increases. This observation suggests that the increase of clay thickness is effective in drier conditions (low degree of saturation) to reduce gas emission rate.

Compared with the gas emission limit set by Australian guideline as shown in the figure, for H = 0.4 m, the requirement for gas emission is only satisfied when the degree of saturation is higher than 40%. However, gas emission rates for H = 0.6 m still stay below it even when the degree of saturation is 10%. In other words, the gas emission rate can be substantially reduced by increasing clay thickness to 0.6 m.

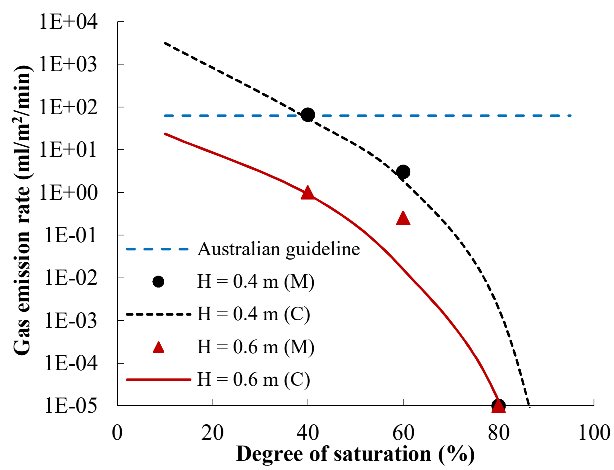

Figure 16 Measured (M) and computed (C) gas emission rates at different degrees of saturation and clay thickness (H) with applied gas pressure of 5 kPa

3.5 Summary and conclusions for earthen cover system

A novel three-layer environmentally friendly earthen cover system was explored and verified for minimizing rainfall infiltration and landfill gas emission under all-weather conditions (Ng et. al. 2015f). The feasibility and effectiveness of the proposed earthen cover system are investigated through theoretical examination using unsaturated soil mechanics and physical modelling (e.g., one-dimensional (1D) soil column and two-dimensional (2D) large flume tests). In addition, numerical back-analysis of the experimental results and parametric studies were carried out by varying water permeability of the clay layer to investigate the effects of cracking on the performance of the three-layer cover system. the following conclusions may be drawn:

1. Both one-dimensional and two-dimensional water infiltration tests show that after water breakthrough of the upper two layers, percolation was prevented by the bottom clay layer for the entire rainfall duration with equivalent rainfall return period of 100 years. This is consistent with the results from numerical simulations that percolation through the proposed cover system was mainly prevented by the clay layer and is found to be the most important component.
2. Based on the numerical parametric study of the water infiltration test, the saturated water permeability of the clay layer should be kept below $1x10^{-8}$ m/s in order to minimize percolation through the proposed cover.
3. Gas breakthrough pressure of unsaturated compacted clay increases as degree of saturation and thickness of clay increase. Under a gas pressure of 10 kPa (the upper bound limit of typical landfill gas pressure), a 0.4 m or thicker clay layer is able to prevent gas breakthrough at degree of saturation of about 60% (e.g. those in humid regions).
4. Gas emission rate tests and numerical simulations show that a clay layer with thickness of 0.6 m compacted at 10% saturation (e.g. those in arid regions) can adequately satisfy the required gas emission rate standard proposed by the Australian guideline.
5. Based on the results of the physical modelling and numerical simulations, it is demonstrated that this newly proposed three-layer landfill cover system can perform satisfactorily in all-weather conditions, without the need of any geomembrane. This new system is thus a promising alternative landfill cover.

4. ACKNOWLEDGEMENTS

The authors would like to acknowledge financial support from the Research Grants Council (RGC) of the HKSAR (HKUST6/CRF/12R, GRF grant no. 617213 and M-HKUST603/13).

5. REFERENCES

Albright, W. H., Benson, C. H., and Gee, G. W. (2004) "Field water balance of landfill covers". Journal of Environmental Quality, 33, Issue 6, pp2317-2332.

Albright, W. H., Benson, C. H., Gee, G. W., Abichou, T., McDonald, E. V., Tyler, S. W., and Rock, S. A. (2006) "Field performance of compacted clay landfill cover at a humid site". Journal of Geotechnical and Geoenvironmental Engineering, 132, Issue 11, pp1393-1403.

Asaoka, A. (1978). "Observational Procedure of Settlement Prediction". Soil and Foundations, 18, Issue 4, pp87-101.

Bi, Y., Wang, X., Liu, Y., Tian, R., Chen, L., & Wu, C. (2009) "Applications of ground source heat pump systems in different temperature zones in China". International Journal of Ambient Energy, 30, Issue 2, pp63–72.

Brandl, H. (2006) "Energy foundations and other thermo-active ground structures". Géotechnique, 56, Issue 2, pp81–122.

Brandl, H. (2016) "Geothermal Geotechnics for Urban Undergrounds". Procedia Engineering, 165, pp747–764.

Bohnhoff, G., Ogorzalek, A., Benson, C., Shackelford, C., and Apiwantragoon, P. (2005) "Field data and water-balance predictions for a monolithic cover in a semiarid climate". Journal of Geotechnical and Geoenvironmental Engineering, 135, Issue 3, pp333-348.

Burland, J. B. (1973) "Shaft Friction of Piles in Clay – A Simple Fundamental Approach". Ground Engineering, 6, Issue 3, pp30-42

CFI (2013) Guidelines for Calculating Regulatory Baselines for Legacy Waste Landfill Methane Projects, Carbon Farming Initiative, Australian Government.

Chen, X. W., Wong, T. F., Mo, W. Y., Man, Y. B., Ng, C. W. W., and Wong, M. H. (2015) "Ecological performance of the restored South East New Territories (SENT) landfill in Hong Kong (2000-2012)". Land Degradation & Development, 27, Issue 6, pp1664-1676.

Coo, J. L., So, Z. P. S., and Ng, C. W. W. (2016) "Effect of nanoparticles on the shrinkage properties of clay". Engineering Geology, 213, pp84-88.

DSD (2013) Stormwater Drainage Manual, Drainage Services Department, Hong Kong.

Energy Efficient Best Practice Programme (EEBPP), (2000). "Heat pumps in UK: current status and activities." General information report 67.

Finnie, I. M. S. (1993) "Performance of Shallow Foundations in Calcareous Soil". PhD Thesis, The University of Western Australia.

Hauser, V. L., Weand, B. L., and Gill, M. D. (2001) "Natural covers for landfills and buried waste". Journal of Environmental Engineering, 127, Issue 9, pp768-775.

Krishnaiah, S. and Singh, D. N. (2004) "Centrifuge modelling of heat migration in soils." International Journal of Physical Modelling in Geotechnics, 4, Issue 3, pp39-47

Lee, L. M., Kassim, A., and Gofar, N. (2011) "Performance of two instrumented laboratory models for the study of rainfall infiltration into unsaturated soils". Engineering Geology, 117, Issue 1-2, pp78-89.

Ma, Q. J., Ng, C. W. W., Mašín, D. and Zhou, C. (2017) "An approach for modelling volume change of fine-grained soil subjected to thermal cycles". Canadian Geotechnical Journal. http://dx.doi.org/10.1139/cgj-2016-0459.

McBean, E. A., Rovers, F. A., and Farquhar, G. J. (1995) Solid Waste Landfill Engineering and Design, Prentice Hall PTR, Englewood Cliffs, New Jersey, pp390-391.

Mualem, Y. (1976) "A new model for predicting the hydraulic conductivity of unsaturated media". Water Resources Research, 12, Issue 3, pp513-522.

Ng, C. W. W., and Pang, Y. W. (2000) "Influence of stress state on soil-water characteristics and slope stability". Journal of Geotechnical and Geoenvironmental Engineering, 126, Issue 2, pp157-166.

Ng, C. W. W., and Menzies, B. (2007) Advanced Unsaturated Soil Mechanics and Engineering, Taylor & Francis, London and NY. ISBN: 978-0-415-43679-3 (Hardcopy). 687p.

Ng, C. W. W. (2014) "The 6th ZENG Guo-xi Lecture: The State-of-the-Art centrifuge modelling of geotechnical problems at HKUST." Journal of Zhejiang University-Science A (Applied Physics & Engineering, 15, Issue 1, pp1-21.

Ng, C. W. W., and Coo, J. L. (2014) "Hydraulic conductivity of clay mixed with nanomaterials". Canadian Geotechnical Journal, 52, Issue 6, pp808-811.

Ng, C. W. W., and Zhou, C. (2014) "Cyclic behaviour of an unsaturated silt at various suctions and temperatures". Géotechnique, 64, Issue 9, pp709–720.

Ng, C. W. W., Shi, C., Gunawan, A., and Laloui, L. (2014) "Centrifuge modelling of energy piles subjected to heating and cooling cycles in clay". Géotechnique Letters, 4, Issue 4, pp310–316.

Ng, C. W. W., Zhou, C., Choi, C. E., and Archer, A. (2015a) The 1st International Conference on Geo-Energy and Geo-Environment, HKUST, PTC, Hong Kong, China, ISBN 978-988-14032-2-3.

Ng, C. W. W., Shi, C., Gunawan, A., Laloui, L., and Liu, H. L. (2015b) "Centrifuge modelling of heating effects on energy pile performance in saturated sand". Canadian Geotechnical Journal, 52, Issue 8, pp1045–1057.

Ng, C. W. W., Liu, J., Chen, R., and Coo, J. L. (2015c) "Numerical parametric study of an alternative three-layer capillary barrier cover system". Environmental Earth Sciences, 74, Issue 5, pp4419-4429.

Ng, C. W. W., Liu, J., and Chen, R. (2015d) "Numerical investigation on gas emission from three landfill soil covers under dry weather conditions". Vadose Zone Journal, 14, Issue 8, pp1-10.

Ng, C. W. W., Feng, S., and Liu, H. W. (2015e) "A fully coupled model for water-gas-heat reactive transport with methane oxidation in landfill covers". Science of the Total Environment, 508, pp307-319.

Ng, C. W. W., Xu, J., and Chen, R. (2015f) "All-weather landfill soil cover system for preventing water infiltration and landfill gas emission". U.S. Patent No. 9,101,968 B2 (granted August 11, 2015).

Ng, C. W. W., Chen, Z. K., Coo, J. L., Chen, R., and Zhou, C. (2015g) "Gas breakthrough and emission through unsaturated compacted clay in landfill final cover". Waste Management, 44, pp155-163.

Ng, C. W. W., Liu, J., Chen, R., and Xu, J. (2015h). "Physical and numerical modeling of an inclined three-layer (silt/gravelly sand/clay) capillary barrier cover system under extreme rainfall". Waste Management, 38, pp210-221.

Ng, C. W. W., Wang, S. H., and Zhou, C. (2016a) "Volume change behaviour of saturated sand under thermal cycles". Géotechnique Letters, 6, Issue 2, pp124–131.

Ng, C. W. W., Cheng, Q., Zhou, C., and Alonso, E. E. (2016b) "Volume changes of an unsaturated clay during heating and cooling". Géotechnique Letters, 6, Issue 3, pp192–198.

Ng, C. W. W., Gunawan, A., Shi, C., Ma, Q. J., and Liu, H. L. (2016) "Centrifuge modelling of displacement and replacement energy piles constructed in saturated sand: A comparative study". Géotechnique Letters, 6, Issue 1, pp34-38.

Ng, C. W. W., Coo, J. L., Chen, Z. K., and Chen, R. (2016d). "Water infiltration into a new three-layer landfill cover system". Journal of Environmental Engineering, 142, Issue 5. http://dx.doi.org/10.1061/(ASCE)EE.1943-7870.0001074.

Ng, C. W. W., Ma, Q. J., and Gunawan, A. (2016e) "Horizontal stress change of energy piles subjected to thermal cycles in sand." Computers and Geotechnics, 78, pp54–61.

Ng, C. W. W., Qing, Y. M., and Zhou, C. (2017a) "Effects of boundary conditions on cyclic thermal strains of clay and sand". Géotechnique Letters, 7, Issue 1, pp1-6.

Ng, C. W. W., Xie, M., and Leung, A. K. (2017b) "Removal of hydrogen sulfide using soil amended with ground granulated blast-furnace slag". Journal of Environmental Engineering, 143, Issue 7. http://dx.doi.org/10.1061/(ASCE)EE.1943-7870.0001206.

Olgun, C. G., & McCartney, J. S. (2014) "Outcomes from international workshop on thermoactive geotechnical systems for near-surface geothermal energy: from research to practice". DFI Journal - The Journal of the Deep Foundations Institute, 8, Issue 2, pp59-73.

Olivella, S., Carrera, J., Gens, A., and Alonso, E. E. (1994) "Non isothermal multiphase flow of brine and gas through saline media". Transport Porous Media, 15, Issue 3, pp271-293.

Omer, A. M. (2008) "Ground-source heat pumps systems and applications." *Renewable and Sustainable Energy Reviews*, *12*, Issue 2, pp344–371.

Parent, S. E., and Cabral, A. (2006) "Design of inclined covers with capillary barrier effect". Geotechnical and Geological Engineering, 24, Issue 3, pp689-710.

Permchart, W., and Tanatvanit, S. (2009) "Study on Using the Ground as A Heat Sink for A 12,000-Btu/h Modified Air Conditioner". World Academy of Science, Engineering and Technology, 3, Issue 3, pp120–123.

Ross, B. (1990) "The diversion capacity of capillary barriers". Water Resources Research, 26, Issue 10, pp2625-2629.

Simons, N. E. and Menzies, B. K. (2000) "A short course in foundation engineering". Taylor & Francis, London and NY.

Soni, S. K., Pandey, M., and Bartaria, V. N. (2016) "Experimental analysis of a direct expansion ground coupled heat exchange system for space cooling requirements". Energy and Buildings, 119, pp85–92.

Shi, C., Van Laak, P. A., Gunawan, A., and Ng, C. W. W. (2015) "Development of a heating and cooling system for centrifuge modelling of energy piles at HKUST", Proceedings of 15th Asian Regional Conference, Fukuoka, Japan, pp2559-2564.

Stormont, J. C., and Anderson, C. E. (1999) "Capillary barrier effect from underlying coarser soil layer". Journal of Geotechnical and Geoenvironmental Engineering, 125, Issue 8, pp641-648.

Tanai, K., Kanno, T., and Gallé, C. (1997) "Experimental study of gas permeabilities and breakthrough pressures in clays". Materials Research Society Symposium Proceedings, 465, pp995-1002.

Taylor, R. N. (2004) "Geotechnical Centrifuge Technology". Taylor & Francis, London and NY.

van Genuchten, M. T. (1980) "A closed-form equation for predicting the hydraulic conductivity of unsaturated soils". Soil Science Society of America Journal, 44, Issue 5, pp892-898.

Weeks, B., and Wilson, G. W. (2005) "Variations in moisture content for a soil cover over a 10 year period". Canadian Geotechnical Journal, 42, Issue 6, pp1615-1630.

Wong, J. T. F., Chen, Z. K., Chen, X. W., Ng, C. W. W., and Wong, M. H. (2017) "Soil-water retention behavior of compacted biochar-amended clay: a novel landfill final cover material". Journal of Soils and Sediments, 17, Issue 3, pp590-598.

Wong, J. T. F., Chen, Z. K., Ng, C. W. W., and Wong, M. H. (2016) "Gas permeability of biochar-amended clay: potential alternative landfill final cover material". Environmental Science and Pollution Research, 23, Issue 8, pp7126-7131.

Xie, M., Leung, A. K., and Ng, C. W. W. (2017) "Mechanisms of hydrogen sulfide removal by ground granulated blast furnace slag amended soil". Chemosphere, 175, pp425-430.

Yang, H., Rahardjo, H., and Leong, E. C. (2006) "Behavior of unsaturated layered soil columns during infiltration". Journal of Hydraulic Engineering, 11, Issue 4, pp329-337.

Zhan, G., Keller, J., Milczarek, M., and Giraudo, J. (2014) "11 years of evapotranspiration cover performance at the AA Leach Pad at Barrick Golstrike mines". Mine Water and the Environment, 33, pp195-205.

Zhou, C. and Ng, C. W. W. (2016) "Simulating the cyclic behaviour of unsaturated soil at various temperatures using a bounding surface model". Géotechnique, 66, Issue 4, pp344-350.

Zornberg, J. G., and McCartney, J. S. (2005) "Evaluation of evapotranspiration from alternative landfill covers at the Rocky Mountain Arsenal", Proceedings of the International Symposium on Advanced Experimental Unsaturated Soil Mechanics, Trento, Italy, pp555-561.